Seminario del Comitato Scientifico dell'Ordine degli Attuari

Addressing the financial impact of natural disasters in the era of climate change

Giuseppe Orlando [1] [2] [*]
giuseppe.orlando@uniba.it

[1]University of Bari - Department of Economics and Finance

[2]HSE University - Department of Economics

[*]Joint work with M. Bufalo and C. Ceci

July 16, 2024

Outline I

Outline II

- Natural catastrophe modeling emerged in the late 1980s after events like Hurricane Andrew and the Northridge earthquake highlighted the need for better risk analysis.

- The frequency and severity of climate-related disasters have exceeded some model predictions, necessitating the development of more accurate techniques.

- Concerns about climate change and insurance premiums stem from uncertainties in estimating reserves and actual losses, compounded by delays in assessing losses.

- Actuarial techniques such as the chain-ladder method are used to estimate incurred but not reported claims and project ultimate loss amounts.

- This presentation is based on the article in Fig. 1.

Addressing the financial impact of natural disasters in the era of climate change

Michele Bufalo [a] ✉ , Claudia Ceci [b] ✉ , Giuseppe Orlando [a] [c] 👤 ✉

Figure 1: Published paper https://doi.org/10.1016/j.najef.2024.102152

Highlights I

- Objective: The study aims to predict (expected and max) financial losses, volatility resulting from natural disasters over a period of 1 to 15 years.

- Volatility Impact: Volatility can cause significant fluctuations in Profit and Loss (P&L) for affected companies due to unexpected events.

- Novelty: A new model for correlating occurrence frequencies with volatility and estimating the maximum potential loss for each specific type of natural disaster.

- Reliability and Comparison: Results were compared to four reference models, and a backtesting analysis was conducted to ensure the reliability of predictions.

- Applicability: Suitable for businesses, such as insurance companies, vulnerable to extreme events, helping them manage risk and ensure stable cash flow.

Outline I

Outline II

Literature review I

- Natural disasters are increasingly frequent and severe due to climate change and population growth Jin et al. (2008).
- Predicting these events is challenging due to their nonlinearity, intermittency, and low correlation Jin et al. (2008).
- Traditional time series analysis tools face limitations in modeling natural disasters due to their non-Gaussian behavior and lack of stationarity Povinelli (2000).
- ARCH/GARCH models are more successful on long-term horizons but may struggle with asymmetric volatility Carbone et al. (2004).
- Point processes like the Hawkes process are used in finance and insurance to model self-exciting events, but they may have limitations in capturing mutual influence, as the Hawkes process assumes linear interactions between events. This means that the impact of past events on future events is assumed to be additive and proportional Bacry et al. (2015); Hawkes (2018).

Literature review II

- Multivariate Hawkes processes, designed to model correlated sequences, may be computationally prohibitive Embrechts et al. (2011); Hall and Willett (2016); Eichler et al. (2017); Shang and Sun (2019).

- Traditional approaches based on geographically located assets and adaptation measures face data issues and require compromise, potentially leading to over- or underestimation of losses Morton and Levy (2011); Lythe et al. (2008); Mitchell-Wallace et al. (2017); Calder et al. (2012).

Outline I

Outline II

Summary of methods and material

- Section 1: Introduction of the dataset used for numerical results.
- Section 2: Hurst exponent
- Section 3: Introduction of the proposed two-factor square-root model for describing the dynamics of log-losses and their volatility.
- Section 4: Forecast of the expected value
- Section 5: Forecast of the extreme value (VaR)
- Section 6: Consideration of popular backtests used for model validation based on VaR exceedances.
- Section 7: Consideration of baseline models for comparison and benchmarking.

Dataset I

- The dataset used is sourced from the Emergency Events Database (EM-DAT) hosted at the Centre for Research on the Epidemiology of Disasters (CRED).

- EM-DAT contains comprehensive data on the occurrence and effects of over 23,000 technological and natural disasters worldwide, spanning from 1900 to the present day.

- The data frequency is on an annual basis.

- The study focuses on losses attributed to five major natural disasters: earthquake, storm, flood, drought, and extreme temperature.

- Figure 2 illustrates the sum of deaths, occurrences, and total damages (in US$) of natural disasters recorded in EM-DAT from 1900 to 2020.

Dataset II
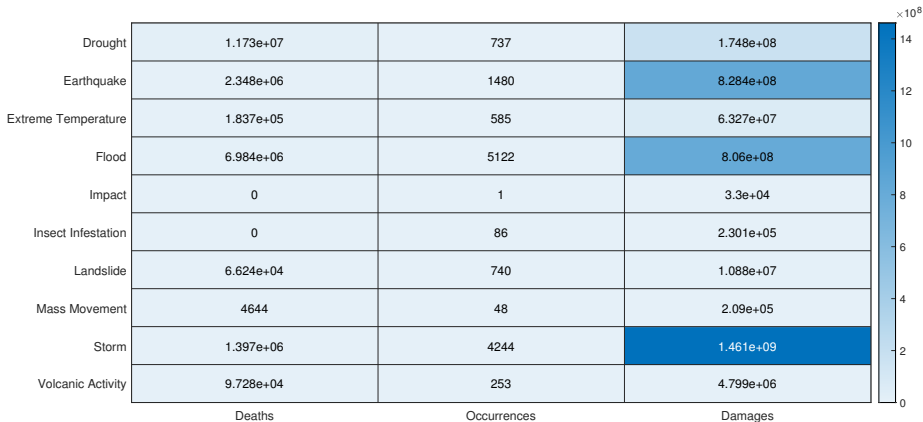
Figure 2: Sum of deaths, occurrences and total damages (US$) of natural disasters (1900-2020).

The data description section outlines the calculation and notation for tracking losses over time. Initially, cumulative losses at each time point are denoted by C_t, where L_h represents the individual loss at time h. To reduce variability in the time series of losses, logarithmic returns are computed using the formula:

$$x_t = \ln\left(\frac{C_t}{C_{t-1}}\right).$$

These logarithmic returns are referred to as "log-losses" for notation purposes.

Hurst exponent I

The Hurst Exponent H helps determine whether a time series is a random walk ($H \approx 0.5$), trending ($H > 0.5$), or mean reverting ($H < 0.5$) for a specific period. In financial markets research, the Hurst Exponent aims to provide a scalar value to identify whether a series is mean reverting, random walking, or trending. The calculation uses the variance of a log price series to assess diffusive behavior. For a time lag τ, the variance is given by:

$$\mathsf{Var}(\tau) = \mathbb{E}[(\log(t + \tau) - \log(t))^2]$$

Comparing the rate of diffusion to geometric Brownian motion, at large τ, the variance is proportional to the time lag:

$$\mathbb{E}[(\log(t + \tau) - \log(t))^2] \sim \tau$$

If autocorrelations exist, this relationship is modified to include an exponent $2H$:

$$\mathbb{E}[(\log(t + \tau) - \log(t))^2] \sim \tau^{2H}$$

Hurst exponent II

Thus, a time series is characterized as:

- $H < 0.5$: Mean reverting
- $H = 0.5$: Geometric Brownian motion
- $H > 0.5$: Trending
- For natural disasters, H is around 0.24, indicating anti-persistence.

A Brownian time series, with no correlation between observations and an estimated Hurst exponent close to 0.5, is unpredictable and exhibits random walk behavior (see Fig. 3).
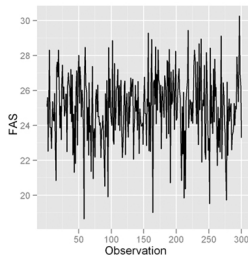
Figure 3: A Brownian time series (H = 0.53). Source Mansukhani (2024)

An anti-persistent time series, or mean-reverting series, tends to revert to a long-term mean, with increases likely followed by decreases and vice-versa, indicated by a Hurst exponent less than 0.5. (see Fig. 4).
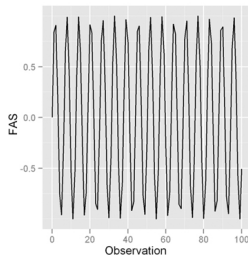
Figure 4: An anti persistent time series (H = 0.043). Source Mansukhani (2024)

A persistent time series is characterized by values that tend to continue in their current direction in the short term, with increases likely followed by further increases and decreases followed by further decreases. This behavior is indicated by a Hurst exponent between 0.5 and 1.0, with larger values signifying stronger trends. Fig. 4 demonstrates this with intra-day tick level data for an NYSE traded fund, showing an estimated Hurst exponent of 0.95.
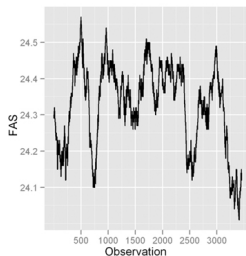
Figure 5: A persistent time series (H = 0.95). Source Mansukhani (2024)

A generalized two-factor square-root model I

Inspired by models used in financial analysis, like Ornstein-Uhlenbeck process for volatility we selected a two-factor square-root model for its features matching natural disaster dynamics.

A generalized two-factor square-root model II

Assume that we are working within a probability space $(\Omega, \mathcal{F}, \{\mathcal{F}_t\}_{t\geq 0}, \mathbb{P})$. This space consists of:

- Ω: The sample space, which is the set of all possible outcomes.
- $\mathcal{F}$: The sigma-algebra, a collection of events for which probabilities can be assigned.
- $\{\mathcal{F}_t\}_{t\geq 0}$: The filtration, which is a sequence of sigma-algebras $\mathcal{F}_t$ that represent the information available up to time t. As time progresses, the filtration $\{\mathcal{F}_t\}_{t\geq 0}$ gets larger, encompassing more information.
- $\mathbb{P}$: The probability measure, which assigns probabilities to the events in $\mathcal{F}$.

In this setting, the dynamics of the processes we study are defined using the filtration $\{\mathcal{F}_t\}_{t\geq 0}$, which helps us understand how information unfolds over time.

A generalized two-factor square-root model III

To introduce our generalized two-factor square-root model, let us start by denoting with $\{x_t\}_{t \geq 0}$ and $\{\sigma_t\}_{t \geq 0}$, respectively, the log-losses process due to natural disasters and the corresponding volatility. Assume that the dynamics of these processes, defined on a given a filtered probability space $(\Omega, \mathcal{F}, \{\mathcal{F}_t\}_{t \geq 0}, \mathbb{P})$, endowed with the filtration $\{\mathcal{F}_t\}_{t \geq 0}$ evolves like a generalized two-factor square-root model defined as follows

$$
\begin{cases}
dx_t = k(\theta - x_t)dt + \alpha\sqrt{|x_t \sigma_t|}\, dW_t^x & x_0 > 0 \\
d\sigma_t = \delta(\gamma - \sigma_t)dt + \eta\sqrt{\sigma_t}\, dW_t^\sigma & \sigma_0 > 0,
\end{cases}
\tag{1}
$$

where $k, \theta, \alpha, \delta, \gamma, \eta$ are strictly positive constants $\{W_t^x\}_{t \geq 0}$ and $\{W_t^\sigma\}_{t \geq 0}$ are two correlated Brownian motions, i.e.

$$
dW_t^x dW_t^\sigma = \rho\, dt \qquad t \geq 0.
$$

and $\rho \in (-1, 1)$. We can write

$$W_t^x = \rho W_t^\sigma + \sqrt{1 - \rho^2}\, B_t, \tag{2}$$

where $\{B_t\}_{t \geq 0}$ is a standard Brownian motion independent of $\{W_t^\sigma\}_{t \geq 0}$. Thus system (1) reads as

$$\begin{cases} dx_t = k(\theta - x_t)dt + \alpha\sqrt{|x_t\sigma_t|}\left(\sqrt{1 - \rho^2}\, dB_t + \rho dW_t^\sigma\right) & x_0 > 0 \\ d\sigma_t = \delta(\gamma - \sigma_t)dt + \eta\sqrt{\sigma_t}\, dW_t^\sigma & \sigma_0 > 0, \end{cases} \tag{3}$$

Forecasting the expected value

Recall that:

- After reviewing existing literature, it is concluded that a two-factor model is most suitable for describing the dynamics of financial log-losses and their volatility.

- The proposed model introduces a nonzero correlation (ρ) between the log-loss (x_t) and volatility (σ_t) processes.

- While more analytically tractable models exist, such as the two-factor Gaussian model, they become unmanageable if ρ is nonzero.

Forecasting the extreme value (VaR)

- Forecasted future values approximate expected values of financial log-losses and volatility well.
- To prevent future observations from exceeding a high level, an upper bound of predictions (x_{t+u}^F) is needed for a 99% confidence level Value at Risk (VaR).
- A correction term (z_{t+u}) is defined to achieve the VaR with a 99% confidence level.
- The correction term (z_{t+u}) ensures the VaR by adjusting the predicted value (x_{t+u}^F) and its volatility (σ_{t+u}^F).
- Extreme values are modeled assuming Z_{t+u} follows a Generalized Pareto Distribution (GPD), a model for tails.
- GPD parameters (ξ, β) are estimated using a rolling window approach with fixed size.
- A realization of the correction term (Z_{t+u}) is estimated using the sample mean of 100,000 simulated random variables with GPD parameters.

To check if a model can meet the expected maximum allowed exceptions, we recur the range of tools available to risk management. We said that the upper bound of the GPD represents the maximum loss. Therefore, similarly to what financial institutions do to backtest their VaR, in the following we describe the most popular methods that we are going to use to validate our model.

- **Traffic Light Test (TLT)** The Traffic Light Test was proposed by the Basel Committee on Banking Supervision 1996, Balthazar (2006) for giving a green light on the adopted model and it is a variant of the binomial test. The TLT test, given a number of exceptions E, calculates the probability of observing from 0 to E exceptions. For instance, if the actual number of exceptions observed in a backtest exceeds the expected threshold, the model may be deemed inadequate.

- **Kupiec's POF Test** This test borrows its name from Kupiec (1995) and it is a variant on the binomial test. The Kupiec test is also named the proportion of failures (POF) test because of how it is constructed. As well as the TLT test, the POF test is based on the binomial distribution but, additionally, it uses a likelihood ratio. This is to check if the probability of exceptions is synchronized with the probability p defined by the VaR confidence level. In case the frequency of exceptions over the backtested time series is different than p, the VaR is rejected.

- **Kupiec's TUFF Tests** Kupiec proposed a second test called time until first failure (TUFF) Jorion et al. (2009). The TUFF test examines the timing of the first failure occurrence. If the first failure occurs too early from a probabilistic standpoint, the VaR is considered rejected by the test. Since examining only the first failure can leave out important information regarding subsequent failures, the TUFF test was designed to consider all recorded failures.

- **Christoffersen's (CC) Interval Forecast Tests** The Interval Forecast Tests, also known as the CC tests, were introduced by Christoffersen (1998). The main concept behind these tests is to evaluate whether the probability of an exception occurring at a specific time is dependent on whether an exception has occurred previously. Unlike the unconditional probability of observing an exception, the CC tests focus solely on the relationship between consecutive time intervals.

Assume we have a time series of daily returns for an investment over 100 days. We have calculated the Value-at-Risk (VaR) at a 95% confidence level, which means we expect exceptions (days where the actual loss exceeds the VaR) to occur 5% of the time.

- $n = 100$ (the number of observations)
- $p = 0.05$ (the expected proportion of exceptions based on the VaR confidence level)
- $x = 8$ (the actual number of exceptions observed in the time series)

The likelihood ratio test statistic is given by:

$$LR_{\text{POF}} = -2 \ln \left(\frac{(1-p)^{n-x} p^x}{(1-\hat{p})^{n-x} \hat{p}^x} \right)$$

where $\hat{p} = \frac{x}{n}$ is the observed proportion of exceptions.

Example on the Kupiec's POF Test II

Substituting the values:

$$n = 100,$$
$$p = 0.05,$$
$$x = 8,$$
$$\hat{p} = \frac{8}{100} = 0.08$$

We get:

$$LR_{\text{POF}} = -2\ln\left(\frac{(1-0.05)^{92} \cdot 0.05^8}{(1-0.08)^{92} \cdot 0.08^8}\right)$$

Calculating the components:

$$(1-0.05)^{92} = 0.95^{92} \approx 0.012$$

$$0.05^8 \approx 3.9 \times 10^{-11}$$

$$(1-0.08)^{92} = 0.92^{92} \approx 0.004$$

$$0.08^8 \approx 1.68 \times 10^{-7}$$

Now we can substitute these into the formula:

$$LR_{\mathsf{POF}} = -2 \ln \left(\frac{0.012 \cdot 3.9 \times 10^{-11}}{0.004 \cdot 1.68 \times 10^{-7}} \right)$$

$$LR_{\mathsf{POF}} = -2 \ln \left(\frac{4.68 \times 10^{-13}}{6.72 \times 10^{-10}} \right)$$

$$LR_{\mathsf{POF}} = -2 \ln \left(6.97 \times 10^{-4} \right)$$

$$LR_{\mathsf{POF}} = -2(-7.27)$$

$$LR_{\mathsf{POF}} \approx 14.54$$

For a significance level of 5%, the critical value from the chi-squared distribution with 1 degree of freedom is approximately 3.84. Since $14.54 > 3.84$, we reject the null hypothesis, indicating that the actual exceptions are not consistent with the expected proportion of 5%, and therefore the VaR model may not be accurate.

In this Section four baseline models for comparison and benchmarking are considered as alternative candidates to system (1) for modelling log-losses of natural disasters. Namely, the first-order autoregressive AR(1) model, the two-factor Gaussian model G2++, the extreme value distribution model (EVM) and the generalized linear regression model (GLM). The AR(1) is pretty good at predicting the average loss and volatility of the stochastic process when more sophisticated models fail. The other three models are often used in insurance and finance for modeling and forecasting stochastic processes as mentioned in Section 8.

The first-order autoregressive AR(1) model

The AR(1) model is a representation of a short-memory random process satisfying the following equation:

$$Y_{t+1} = c + \Phi Y_t + \varepsilon_{t+1},$$

with c a given constant. The output random variable Y_{t+1} is assumed to depend linearly only on its previous value Y_t and on the current value of a white noise process ε_t with zero mean and constant variance $\sigma_\varepsilon^2 > 0$. The process is stationary if the parameter $\Phi \in (0, 1)$.

The G2++ model

The G2++ model is a two-factor Gaussian model where the state process is the sum of two correlated Gaussian factors plus a deterministic function chosen to fit the observed real data exactly. Due to its analytic tractability, explicit formulas for its distribution and moments can be easily derived. Gaussian models, such as the G2++, are widely used in practice due to their practical usefulness. For more details see (Brigo and Mercurio, 2006, Chapter IV).

Under this model, the principal process Y_t is expressed as the sum

$$Y_t = r_t + q_t + \varphi(t),$$

where the processes $\{r_t\}_{t\geq0}$ and $\{q_t\}_{t\geq0}$ satisfy

$$\begin{cases} dr_t = -a\, r_t dt + \psi\, dW_t^r & r_0 > 0 \\ dq_t = -b\, q\, dt + \zeta\, dW_t^q, & q_0 > 0 \end{cases} \tag{4}$$

with $\{W_t^r\}_{t\geq0}$, $\{W_t^q\}_{t\geq0}$ correlated Brownian motion such that $dW_t^r dW_t^q = \rho\, dt$, $\rho \in (-1,1)$ and a, ψ, b, ζ are positive constants.

The extreme value distribution model (EVM)

Extreme value distributions are widely used in finance because they can effectively model extreme events that cannot be represented by other distributions such as the Gaussian, which has tails that decay exponentially quickly.

Given the location parameter a_1 and scale parameter a_2, the probability density function for the extreme value distribution

$$y = f(x|a_1, a_2) = \frac{1}{a_2} e^{(x-a_1)/a_2 - e^{(x-a_1)/a_2}}.$$

It can be observed that if X has a Weibull distribution with parameters $b_1 > 0$ and $b_2 > 0$, then $\log X$ has an extreme value distribution with parameters $a_1 = \log b_1$ and $a_2 = 1/b_2$.

Generalized linear model (GLM)

The last baseline model that we introduce for comparison is the generalized linear model (GLM) that we use for nonlinear prediction (NLP)

$$y = c_1 + c_2 e^{-c_3 x} \tag{5}$$

where c_1, c_2 and c_3 are some parameters we calibrate by means of a nonlinear least squares regression. Eq. (5) is consistent with the G2++, is an industry standard (see De Jong and Heller (2008); Ohlsson and Johansson (2010); Goldburd et al. (2016)) and, in our tests, performed well in fitting data. We have run a robust estimation with the iteratively reweighted least squares algorithm Holland and Welsch (1977) which, at each iteration, recalculates the weights based on the residual from the previous iteration. This process progressively downweights outliers and iterations continue until the weights converge.

As a measure of accuracy we adopt the following statistics:

- The root mean squared error (RMSE), defined as

$$RMSE = \sqrt{\frac{1}{N} \sum_{h=1}^{N} e_h^2}, \tag{6}$$

  with e_h representing the residuals between the observed data and their corresponding predictions, computed over N observations. The residual term reflects how close the predicted values are to the actual observed data, where values close to zero indicate a good match, and values close to one indicate poor performance. To mitigate the impact of outliers, the normalized root mean squared error (NRMSE) is used instead. This is defined as follows

$$NRMSE = \frac{RMSE}{X_{max} - X_{min}}, \tag{7}$$

  where X_{max} and X_{min} are the maximum and minimum value of the historical time series, respectively.

- The mean absolute percentage error (MAPE), defined below

$$MAPE = \frac{1}{N} \sum_{h=1}^{N} \left| \frac{e_h}{X_h} \right|. \tag{8}$$

Outline I

Outline II

- Results on 5, 10 and 15-year horizon

5 Conclusions

Example on earthquake forecasts I

In the figure shown in Fig. 6, the log losses of a natural disaster are represented by a dotted black line. This line exhibits erratic and unpredictable behavior, which poses a challenge for insurers who aim to estimate the expected losses over time. To address this challenge, a simple moving average (SMA) is calculated based on the realized occurrences of losses and is represented by the blue line. Note that in our method, the SMA includes 20 points, as determined by the rolling window size set to $L' = 20$. Initially calibrated with $L = 10$ (equivalent to ten years), we progressively increase L by one each subsequent year (i.e., with each data point) until it reaches 20. In addition, the forecasts calculated with Eq. 1 (red line) and upper bound (green line) are shown. The upper bound represents the value at risk (VaR) for the model used (described in Section 5) and is obtained using the generalized Pareto distribution (GPD) and the methodology outlined before. The graph illustrates that the model is very close to the SMA and, except for one exception over 119 years, consistently predicts losses that are higher than the peaks of realized losses.

Figure 6: Earthquake Forecasts. The (dotted) black line is the log-losses of the natural disaster X_t, the blue line is its SMA (ex post), the red line represents the corresponding forecasts x_t^F; finally the green line refers to the upper bound VaR_{GPD} computed as $x_t^F + \sigma_t^F + Z_t$ with $L' = 119$. Out of sample forecasts.

In addition to evaluating the logarithmic losses, we intend to estimate their average volatility. This is of particular importance from a firm standpoint as the aim, is not only to ensure solvency but, also, to deliver a regular stream of cash flow to the shareholders by avoiding excessive variations due to reserves' volatility. Figure 7 presents a comparison between the average ex-post volatility of logarithmic losses, represented by the simple moving average (SMA) in blue, and our ex-ante forecast in red. As can be observed, our forecast is in good agreement with the realized volatility, which provides support to the accuracy of our model.
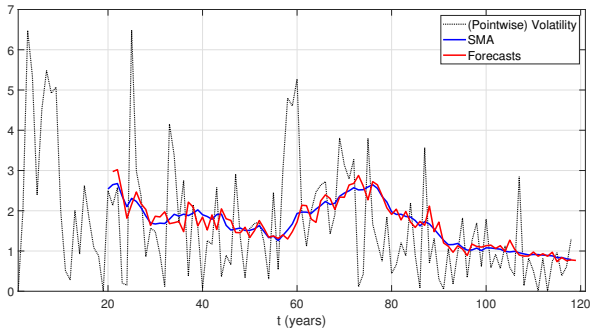
Figure 7: Earthquake volatility Forecasts. The black (dotted) line is the (pointwise) volatility of the log-losses of disaster V_t, the blue line is its SMA (ex post), the red line represents the corresponding forecasts σ_t^F.

In this section we provide an overview of the findings from applying a specific procedure to a dataset, with references to relevant sections for details. The procedure involves computing NRMSE and MAPE for forecasted financial log losses and volatility. The results are compared with baseline models like AR(1) and SMA, which are typically used for forecasting smooth time series. The calibration of the G2++ model is described, focusing on variations rather than levels to control them and avoid unexpected large losses for insurers. Formulas for predicting expected log-losses and volatility are referenced.

Results on 1-year horizon II

Forecasting error of considered models - Returns					
Horizon	**Model Error**	**Earthquake**	**Storm**	**Flood**	**Drought**	**Ext. Temp.**
	$\text{NRMSE}_{Eq.(1)}$	3.32%	4.80%	4.92%	4.54%	2.44%
	NRMSE_{AR}	24.14%	20.18%	14.30%	17.55%	9.10%
1 Y	NRMSE_{G2}	19.30%	12.46%	15.98%	19.05%	11.21%
	NRMSE_{EVM}	5.79%	4.48%	4.9%	19.05%	10.21%
	NRMSE_{GLM}	17.12%	5.94%	5.36%	7.18%	2.99%
	$\text{MAPE}_{Eq.(1)}$	4.77%	3.02%	5.87%	6.67%	3.02%
	MAPE_{AR}	6.59%	7.14%	18.24%	20.77%	12.16%
1 Y	MAPE_{G2}	7.66%	8.42%	22.78%	21.58%	14.34%
	MAPE_{EVM}	5.23%	3.13%	9.01%	10.23%	6.57%
	MAPE_{GLM}	8.01%	4.20%	13.35%	6.70%	2.91%

Table 1: NRMSE and MAPE between 1 year forecasts of log-losses and their SMA. The gray highlights the results obtained with model in Eq. (1). Out of sample results.

Forecasting error of considered models - Volatility					
Horizon	**Model Error**	**Earthquake**	**Storm**	**Flood**	**Drought**	**Ext. Temp.**
	$\text{NRMSE}_{Eq.(1)}$	8.76%	9.24%	6.55%	9.85%	5.19%
	NRMSE_{AR}	53.10%	37.35%	18.77%	39.43%	44.56%
1 Y	NRMSE_{G2}	24.73%	13.75%	25.48%	45.63%	20.61%
	NRMSE_{EVM}	11.74%	8.49%	6.01%	9.6%	28.80%
	NRMSE_{GLM}	30.12%	24.52%	23.07%	33.45%	23.16%
	$\text{MAPE}_{Eq.(1)}$	5.10%	3.62%	3.60%	7.25%	2.88%
	MAPE_{AR}	11.48%	12.07%	11.13%	20.98%	26.88%
1 Y	MAPE_{G2}	12.13%	11.74%	20.68%	28.94%	10.50%
	MAPE_{EVM}	12.04%	11.71%	8.91%	14.23%	16.72%
	MAPE_{GLM}	35.27%	33.20%	31.31%	48.27%	38.19%

Table 2: NRMSE and MAPE between 1 year forecasts of volatility of log-losses and their SMA. The gray highlights the results obtained with model in Eq. (1). Out of sample results.

The verification of whether the correction term Z_t provides a Value at Risk (VaR) at a 99% confidence level involves examining the percentage variation of the exceedances for all time steps beyond a certain window size. By analyzing these variations and exceedances for different window sizes ($L' \geq 20$), the smoothness of hedging for insurance companies can be determined.

The Kupiec (POF), Christoffersen (CC), and TUFF tests do not reject their null hypotheses at a 99% significance level. The corresponding p-values and L-ratios are detailed in Table 3. Notably, these statistical measures are consistent across different time series due to identical numbers of observations, exceedances, and relative frequencies.

Moreover, the traffic light test results in a "green" categorization, indicating a cumulative probability of failures of 1.6%.

- Statistical tests:
  - Kupiec (POF), Christoffersen (CC), and TUFF tests.
  - Non-rejection of null hypotheses at 99% significance level.
  - p-values and L-ratios provided in Table 3.
- Traffic light test result:
  - "Green" category classification.
  - Cumulative probability of failures: 1.6%.

	POF	CC	TUFF, TBFI
Response	"accept"	"accept"	"accept"
p-value	0.1542	0.3623	0.4297
L-ratio	2.0301	2.0301	4.0964

Table 3: 99% VaR test response. Out of sample results.

In addition to 1-year forecasts, to highlight the power of our predictions, we apply the analysis to the next $5Y$, $10Y$ and $15Y$ horizons. As previously done, all forecasts are out of sample. We start with a window of ten data (from $T = 10Y$) and the results are listed in Table 4.

For the reason of space, graphs are in Bufalo et al. (2024), where we show the forecasted series (relative to the next year or 5, 10 and 15 years) $x_{t+u}^F, \sigma_{t+u}^F$ and the percentage variation of Z_t for any natural disaster considered.

Forecasting error of considered models - Returns					
Horizon	Model Error	Earthquake	Storm	Flood	Drought	Ext. Temp.
	$\text{MAPE}_{Eq.(1)}$	5.10%	6.23%	12.68%	20.60%	20.01%
	MAPE_{AR}	15.46%	14.68%	29.75%	34.34%	22.52%
5 Y	MAPE_{G2}	7.79%	8.45%	23.01%	26.70%	20.91%
	MAPE_{EVM}	5.91%	8.03%	22.73%	22.12%	20.84%
	MAPE_{GLM}	6.90%	7.88%	30.84%	24.37%	12.25%
	$\text{MAPE}_{Eq.(1)}$	5.32%	7.95%	17.60%	29.45%	21.45%
	MAPE_{AR}	16.46%	18.19%	28.75%	38.50%	54.05%
10 Y	MAPE_{G2}	7.90%	10.15%	26.59%	29.70%	25.25%
	MAPE_{EVM}	9.16%	12.85%	29.77%	36.91%	23.25%
	MAPE_{GLM}	11.23%	14.49%	46.64%	34.14%	23.95%
	$\text{MAPE}_{Eq.(1)}$	6.72%	10.25%	19.69%	32.68%	25.15%
	MAPE_{AR}	18.46%	22.19%	29.84%	42.04%	56.27%
15 Y	MAPE_{G2}	9.30%	10.92%	27.09%	39.70%	29.34%
	MAPE_{EVM}	11.14%	16.63%	31.99%	38.31%	26.11%
	MAPE_{GLM}	14.47%	28.97%	48.29%	35.42%	39.14%

Table 4: Different MAPE for 5, 10 and 15 years predictions. The gray highlights the results obtained with model in Eq. (1). Out of sample results.

Notice that, as well as illustrated in Tables 1 and 2, we obtained similar results with regard to the volatility and the NRMSE. For the sake of readability, we do not show those results.

Finally, Table 5 shows the ML estimates with their confidence intervals.

Parameter	Estimation	Confidence interval
δ	11.1052	[8.4354, 13.7750]
γ	1.9818	[1.6601, 2.3036]
η	6.4060	[5.6240, 7.1880]
k	1.0422	[0.9830, 1.1014]
θ	11.0976	[10.5315, 11.6637]
α	4.2469	[3.7285, 4.7653]

Table 5: Earthquake simulations. Parameters estimations and their confidence intervals.

Outline I

Outline II

- Results on 5, 10 and 15-year horizon

5. **Conclusions**

Conclusions I

- Introduction of an innovative model for predicting expected losses and volatility resulting from natural disasters over 1, 5, 10, and 15 years.
- Model based on a generalized two-factor square-root approach incorporating stochastic correlation via Brownian motion.
- Utilization of Generalized Pareto Distribution (GPD) to estimate maximum potential losses (VaR) due to extreme claims.
- Comparison of model accuracy with four baseline models: AR, G2++, EVM, and GLM.
- Evaluation of model performance through backtesting exceedances over forecasted VaR, validating the chosen approach.
- Addressing deficiencies in Catastrophe Bond Pricing Models (CBPM) related to GEV, trigger model intricacies, ARIMA limitations, and CIR inefficacy.
- Emphasis on mitigating moral hazard for investors near the trigger, highlighting the importance of transparent catastrophe bond pricing models.

- Application of the methodology to estimate insurance premiums related to dramatic changes in specific lines of business (LOB) triggered by events like COVID-19.

- Contribution to the development of accurate and transparent earthquake catastrophe bond pricing models, meeting market demands.

References I

Bacry, E., Mastromatteo, I., and Muzy, J.-F. (2015). Hawkes processes in finance. *Market Microstructure and Liquidity*, 1(01):1550005.

Balthazar, L. (2006). The regulation of market risk: The 1996 amendment. In *From Basel 1 to Basel 3: The Integration of State-of-the-Art Risk Modeling in Banking Regulation*, pages 23–31. Springer.

Basel Committee (1996). Supervisory framework for the use of backtesting in conjunction with the internal models approach to market risk capital requirements. *Basel Committee on Banking and Supervision, Switzerland*.

Brigo, D. and Mercurio, F. (2006). *Interest rate models-theory and practice: with smile, inflation and credit*. Springer-Verlag: Berlin, Heidelberg.

Bufalo, M., Ceci, C., and Orlando, G. (2024). Addressing the financial impact of natural disasters in the era of climate change. *North American Journal of Economics and Finance*, 73:102152.

Calder, A., Couper, A., Lo, J., and Aspen, P. (2012). Catastrophe model blending techniques and governance.

References II

Carbone, A., Castelli, G., and Stanley, H. E. (2004). Time-dependent hurst exponent in financial time series. *Physica A: Statistical Mechanics and its Applications*, 344(1-2):267–271.

Christoffersen, P. F. (1998). Evaluating interval forecasts. *International economic review*, pages 841–862.

De Jong, P. and Heller, G. Z. (2008). *Generalized linear models for insurance data*. Cambridge University Press.

Eichler, M., Dahlhaus, R., and Dueck, J. (2017). Graphical modeling for multivariate Hawkes processes with nonparametric link functions. *Journal of Time Series Analysis*, 38(2):225–242.

Embrechts, P., Liniger, T., and Lin, L. (2011). Multivariate Hawkes processes: an application to financial data. *Journal of Applied Probability*, 48(A):367–378.

Goldburd, M., Khare, A., and Tevet, D. (2016). *Generalized linear models for insurance rating*. Number 5. Casualty Actuarial Society, CAS Monographs Series.

Hall, E. C. and Willett, R. M. (2016). Tracking dynamic point processes on networks. *IEEE Transactions on Information Theory*, 62(7):4327–4346.

Hawkes, A. G. (2018). Hawkes processes and their applications to finance: a review. *Quantitative Finance*, 18(2):193–198.

Holland, P. W. and Welsch, R. E. (1977). Robust regression using iteratively reweighted least-squares. *Communications in Statistics-theory and Methods*, 6(9):813–827.

Jin, J.-L., Cheng, J., and Wei, Y.-M. (2008). Forecasting flood disasters using an accelerated genetic algorithm: Examples of two case studies for China. *Natural Hazards*, 44(1):85–92.

Jorion, P. et al. (2009). *Financial risk manager handbook*, volume 406. John Wiley & Sons.

Kupiec, P. (1995). Techniques for verifying the accuracy of risk measurement models. *The Journal of Derivatives*, 3(2).

Lythe, R., Shah, Hemant, L., and Grossi, P. (2008). A Guide to Catastrophe Modelling.

Mansukhani, S. (2024). The Hurst Exponent: Predictability of Time Series. *Analytics Magazine*. [Online; accessed 16. Jul. 2024].

Mitchell-Wallace, K., Jones, M., Hillier, J., and Foote, M. (2017). *Natural catastrophe risk management and modelling: A practitioner's guide*. John Wiley & Sons.

Morton, M. and Levy, J. L. (2011). Challenges in Disaster Data Collection during Recent Disasters. *Prehospital Disaster Med.*, 26(3):196–201.

Ohlsson, E. and Johansson, B. (2010). *Non-life insurance pricing with generalized linear models*, volume 174. Springer.

Povinelli, R. J. (2000). Identifying temporal patterns for characterization and prediction of financial time series events. In *International Workshop on Temporal, Spatial, and Spatio-Temporal Data Mining*, pages 46–61. Springer.

Shang, J. and Sun, M. (2019). Geometric Hawkes processes with graph convolutional recurrent neural networks. In *Proceedings of the AAAI Conference on Artificial Intelligence*, volume 33, pages 4878–4885.